Journal of Natural Science Review

Vol. 2, No. 3, 2024, 97-120
https://kujnsr.com
e-ISSN: 3006-7804

Modeling the Transmission Dynamics of the Ebola Virus: Effects of Quarantine and Vaccination

Wahidullah Zgham[1], Sarojkumar Sahani[2], Hezbullah Rahimi[3]✉

[1,2]Faculty of Mathematics and Computer Science, South Asian University, New Delhi, India
[3] Faculty of Mathematics, Kabul University, Afghanistan

✉E-mail: hezbullah.rahimi2024@gmail.com (corresponding author)

ABSTRACT

Quarantine and vaccination of individuals suspected of exposure to infectious agents are fundamental public health strategies that have historically been employed to mitigate the transmission of contagious diseases within human populations. This study introduced a modified SEIVQRD deterministic model to evaluate the population-level effects of quarantine and vaccination on individuals potentially exposed to the Ebola virus. The study showed that the Model exhibits backward bifurcation when $\mathcal{R}_0 = 1$. This implies that even when the reproductive number $\mathcal{R}_0$ An unstable endemic and a stable disease-free equilibrium can coexist in less than one. This phenomenon arises from imperfect quarantine and indicates that while $\mathcal{R}_0 < 1$ is necessary for adequate infection control; it is no longer sufficient and creates additional challenges for effectively controlling Ebola. Furthermore, the sensitivity analysis revealed that the quarantine effectiveness parameter and the parameter related to the isolation of vulnerable individuals had less influence on the incidence of new Ebola cases. However, vaccinating non-quarantined susceptible individuals significantly affects the infection burden and can lower the reproductive value to less than one. Overall, the Model emphasizes the critical role of vaccination in reducing Ebola virus transmission. Although quarantine measures alone may not be sufficient, their combination with vaccination can significantly reduce infection rates.

ARTICLE INFO

Article history:
Received: August 10, 2024
Revised: August 27, 2024
Accepted: September 10, 2024

Keywords: Backward bifurcation; Vaccination strategies; Ebola epidemic dynamics; Quarantine implementation; Stability analysis

To cite this article: Zgham, W. Sahani, S., & Rahimi, H. (2024). Modeling the Transmission Dynamics of the Ebola Virus: Effects of Quarantine and Vaccination. *Journal of Natural Science Review*, *2*(3), 97-120. DOI: https://doi.org/10.62810/jnsr.v2i3.88

To link to this article: https://kujnsr.com/JNSR/article/view/88

INTRODUCTION

Historically, contagious diseases have posed a significant risk to global health, causing widespread morbidity and mortality (Rai et al., 2024). Ancient outbreaks such as the Spanish flu and Black Death Bubonic Plague have caused tens of millions of deaths. In modern times, diseases such as measles, malaria, tuberculosis, and AIDS (acquired immunodeficiency syndrome) continue to cause millions of deaths annually, highlighting the persistent burden of infectious diseases on public health (Desai & Arora, 2023). The global increase in infectious diseases, such as COVID-19, cholera, dengue, and influenza, underscores the importance of

monitoring and reporting disease outbreaks to implement effective control strategies and warning systems (Maldonado, 2023). Education and public awareness campaigns, particularly those promoting hygienic and healthy lifestyles, play a significant role in decreasing the prevalence of diseases caused by infectious microorganisms, including bacteria, viruses, fungi, and parasites (Siddique, 2022).

Ebola virus disease (EVD) is a severe and frequently fatal infection, with case fatality rates ranging from 25% to 90% (Bisimwa et al., 2022; Science et al., 2023). The virus was discovered in Zaire in 1976 (Sabaté, 2021). Disease symptoms include fever, throat pain, muscular discomfort, headaches, vomiting, diarrhea, rash, and internal and external bleeding (Science et al., 2023). The incubation period for the disease ranges from two to twenty-one days (Sabaté, 2021). EVD mainly spreads through contact with infected individuals' blood, bodily fluids, or tissue (Jain et al. & Science et al., 2023). The largest outbreak of Ebola began in Guinea in December 2013, infecting 29,000 individuals and resulting in over 11,000 deaths in Sierra Leone, Liberia, and Guinea (Samadi, 2024; Umutesi et al., 2023). A recent epidemic in Congo in April 2018 caused 237 cases and 153 deaths as of October 20, 2018 (Sabaté, 2021). Surveillance, early detection, and proper public health measures are essential for controlling the propagation of EVD and minimizing its effects on the affected populations (Isiaka et al., 2024).

Mathematical models, such as compartmental models, are critical for comprehending and forecasting the propagation of infectious diseases such as tuberculosis (TB) and COVID-19 (Castillo-Chavez & Song, 2004). These models provide an analytical framework for studying population outbreak dynamics by inferring transmission patterns, forecasting future trends, and analysing prediction uncertainty (Dubey et al., 2016; Marino et al., 2008.). By dividing populations into compartments based on disease stages, these models help to analyse disease severity and accurately predict the spread of infections (Biology Methods & Protocols, 2023). Moreover, advancements in modelling techniques, such as the modified susceptible-infected-recovered (SIR) Model and the use of network effects, have enhanced our understanding of how an infection can move through a network of individuals (percolation phenomena) and herd immunity, contributing to more effective epidemic management strategies (Harris & Bodmann, 2022).

Recent research on EVD transmission dynamics has highlighted the importance of quarantine and vaccination for limiting EVD outbreaks (Ria Rai et al., 2024). Studies have shown that implementing appropriate quarantine measures for exposed persons can considerably minimize the spread of EVD. In contrast, vaccination programs have been demonstrated to prevent an epidemic of infections when the fundamental reproductive value is smaller than one (Abayomi et al., 2023). Additionally, the persistence of EVD in body fluids post-recovery underscores the necessity for close monitoring of survivors and contacts to prevent re-emergence of the disease (Liu et al., 2022). Furthermore, the availability of hospital beds and refurbishment of uninhabitable beds are critical factors in EVD outbreaks,

emphasizing the need for continuous resource management in healthcare facilities (Pecoraro et al., 2021).

In this study, we developed a deterministic mathematical model of SEIQRD presented by Dénes et al. (2019). Our Model introduces two new compartments for vaccinated individuals: one for those who are not quarantined and the other for those who are quarantined. Unlike the Model demonstrated by (Dénes et al., 2019), which uses a standard incidence rate of infection (for quarantined individuals), we employed a monotone nonlinear incidence rate (Crowley-Martin type). This approach models the rate at which new cases occur over time rather than the cumulative number of cases, thereby accounting for the inhibitory effects of behavioural changes among susceptible and infected individuals as their numbers increase. This modification addresses the discontinuity issue found in the right-hand side function of the Model at the disease-free equilibrium point, making it necessary for accurate representation.

This study aimed to develop and analyse a model of Ebola virus transmission dynamics, focusing on assessing the impact of quarantine and vaccination measures on disease control. Specifically, this study aimed to:

1. **Analyse the stability of the disease-free equilibrium (DFE)**: evaluate how the primary reproductive number (R_0) affects the stability of the DFE and identify the conditions under which the DFE remains stable.
2. **Investigate backward bifurcation**: Examine the occurrence of backward bifurcation and its implications for disease persistence, especially in contexts where quarantine measures are imperfect and vaccination coverage varies.
3. **Determine the non-existence of backward bifurcation**: Investigate the conditions under which backward bifurcation does not occur, providing insights into scenarios where disease eradication is more achievable.
4. **Conduct uncertainty and sensitivity analysis**: Assess the impact of parameter uncertainties and sensitivities on the Model's predictions to gauge the robustness of the proposed control strategies.
5. Numerical simulations were performed to validate the theoretical findings and investigate the practical implications of quarantine and vaccination strategies for controlling Ebola virus transmission.

METHODS AND MATERIALS

The Model is constructed as follows. The total number of people, $N(t)$, at time t is divided into two groups: non-quarantined persons $N_U(t)$ and quarantined persons $N_Q(t)$. Thus, $N(t) = N_Q(t) + N_U(t)$ the quarantined individuals are further categorized into four classes: Susceptible, Exposed, Vaccinated, and Symptomatic, denoted by $S_Q(t)$, $E_Q(t)$, $V_Q(t)$ and I_Q, respectively. Therefore,

$$N_Q(t) = S_Q(t) + E_Q(t) + V_Q(t) + I_Q(t). \tag{1}$$

Similarly, at time t, the total non-quarantined persons are split into the $S_U(t)$ (susceptible), $E_U(t)$ (exposed, which are infected but still not infectious), $V_U(t)$ (vaccinated), $I_U(t)$ (symptomatic), $I_T(t)$ (treated), $R(t)$ (recovered), $D(t)$ (dead) classes. Hence

$$N_U(t) = S_U(t) + E_U(t) + V_U(t) + I_U(t) + I_T(t) + R(t) + D(t).$$

The force of infection related to the Model (denoted by $\lambda(t)$) is calculated as (Dénes et al., 2019):

$$\lambda(t) = \frac{I_U(t) + \eta_T I_T(t) + \eta_Q I_Q(t) + \eta_D D(t)}{N_U(t)} \tag{2}$$

In equation (2), the contagiousness of people in the I_T, I_Q, and D categories are adjusted by the parameters η_T, η_Q, and η_D, respectively. This adjustment reflects their relative infectiousness compared to that of the $I_U(t)$ (symptomatic) class. Similar to the approach in reference (Dénes et al., 2019.), quarantine is modelled as follows:

Susceptible individuals suspected of having Ebola are quarantined at a rate q. Due to imperfections in quarantine, there is a probability b that quarantined individuals may become infected and proceed to the E_Q Category. Simultaneously, quarantined people remain in S_Q Class of susceptible individuals, with a probability of $(1-b)$, remain susceptible. Additionally, at the rate r_Q, quarantined susceptible individuals are transferred to the S_U Class, where they did not become infected by completing the quarantine phase.

In the Model described by (Brettin et al., 2018), vaccination was implemented as follows: The rate. ϕ_1 of individuals from the un-quarantined susceptible class S_U is vaccinated and moved to the vaccinated class V_U. Similarly, a rate ϕ_2 of individuals from the quarantined susceptible class S_Q are vaccinated and transferred to the vaccinated class V_Q. We assumed that the effectiveness of vaccination decreases over time at a rate of ω for individuals in both V_U and V_Q. Figure 1 illustrates the flow diagram of the Model, and Table 1 lists its parameters.

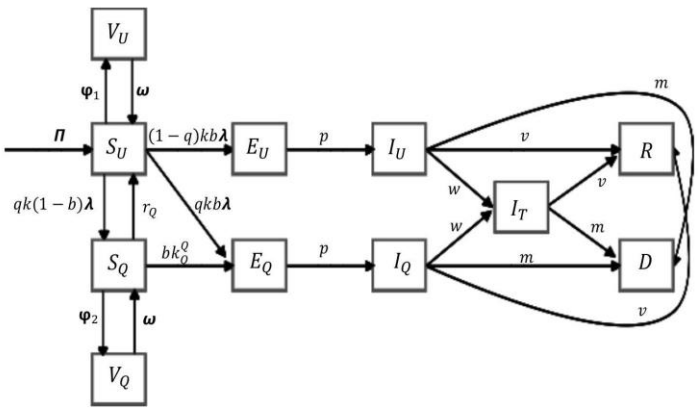

Figure 1. Flow diagram of model 3

A system of deterministic nonlinear differential equations represents the Model.

$$
\begin{aligned}
S_U'(t) &= \Pi - kbS_U(t)\lambda(t) - qk(1-b)S_U(t)\lambda(t) + r_Q S_Q(t) - \phi_1 S_U(t) + \omega V_U(t) \\
&\quad -dS_U(t) \\
S_Q'(t) &= qk(1-b)S_U(t)\lambda(t) - \frac{bk_Q^Q S_Q(t) I_Q(t)}{\big(1+\alpha_1 S_Q(t)\big)\big(1+\alpha_2 I_Q(t)\big)} - r_Q S_Q(t) - \phi_2 S_Q(t) \\
&\quad +\omega V_Q(t) - dS_Q(t) \\
E_U'(t) &= (1-q)kbS_U(t)\lambda(t) - pE_U(t) - dE_U(t) \\
E_Q'(t) &= qkbS_U(t)\lambda(t) + \frac{bk_Q^Q S_Q(t) I_Q(t)}{\big(1+\alpha_1 S_Q(t)\big)\big(1+\alpha_2 I_Q(t)\big)} - pE_Q(t) - dE_Q(t) \\
V_U'(t) &= \phi_1 S_U(t) - \omega V_U(t) - dV_U(t) \\
V_Q'(t) &= \phi_2 S_Q(t) - \omega V_Q(t) - dV_Q(t) \\
I_U'(t) &= pE_U(t) - (v+m+w)I_U(t) - dI_U(t) \\
I_T'(t) &= w\big(I_U(t) + I_Q(t)\big) - (v+m)I_T(t) - dI_T(t) \\
I_Q'(t) &= pE_Q(t) - (v+m+w)I_Q(t) - dI_Q(t) \\
R'(t) &= v\big(I_U(t) + I_T(t) + I_Q(t)\big) - dR(t) \\
D'(t) &= m\big(I_U(t) + I_T(t) + I_Q(t)\big) - fD(t)
\end{aligned}
\tag{3}
$$

The auxiliary equation for model (2) is given by

$$B'(t) = fD(t) \tag{4}$$

Π represents the recruitment rate due to immigration or childbirth. The likelihood of infection for each contact is denoted by b, and the average daily rate of interactions between people is represented by k. The infection force of the Model, denoted by $\lambda(t)$, is defined by Equation (2). Instead of using the usual combined transfer parameter β, we separate the parameters b and k. This means we assume that a proportion b of the k contacts made by an infectious person each day leads to infection. Parameter q represents the proportion of vulnerable people quarantined, and the natural rate is denoted by d. This mortality proportion was presumed to be uniform across all categories. Quarantined people contract the Ebola virus in a proportion of bk_Q^Q. Parameters ϕ_1 and ϕ_2 represent the vaccination rates for non-quarantined and quarantined susceptible individuals, respectively, and ω is the wear-off rate.

Parameter p indicates the proportion of people who progressed from the exposed categories (I_U or I_Q) to the symptomatic categories (E_U or E_Q). Specifically, the mean incubation time for infection is $1/p$. Parameter w represents the proportion of hospitalized infectious people in symptomatic categories I_U and I_Q. Parameter v indicates the proportion at which infected people recover, whereas m represents the per capita death proportion caused by the infection. Parameter f is the burial rate for individuals who have died from

Ebola, meaning that the average time from death to burial is $1/f$. Hospitalized individuals are believed to transmit the disease. The mean infectiousness period is $(1/w + m + v)$.

As mentioned by (Dénes et al., 2019), Model (3) improves upon several existing quarantine and isolation models by incorporating a nonlinear rate for quarantining susceptible individuals, which allows infection rates to increase even during quarantine. Additionally, we applied the monotone (Crowley-Martin type) incidence rate for infections during quarantine, which permits infected individuals to continue transmitting the infection while quarantined or isolated. This Model accounts for the heterogeneity between infected individuals who are quarantined or isolated and those who are not. Specifically, it distinguishes infected people based on whether they are quarantined or isolated (E_Q and I_Q) and those who are neither quarantined nor isolated (E_U and I_U). This approach facilitates the evaluation of intervention strategies to promote behavioural changes among infected individuals in quarantine or isolation, thereby reducing the transmission of infections.

Table 1. Description of parameters, their baseline values, and ranges

Description of parameters	Range	Reference
Π Rate of recruitment	$11826/week$	(Dénes et al., 2019.)
d Rate of natural death	$0.00054/\ week$	(Dénes et al., 2019.)
b Probability of transmission per contact	0.054	(Dénes et al., 2019.)
η_T Modifies the transmissibility of hospitalized people	0.86	(Dénes et al., 2019.)
η_Q Modifies the infectiousness of quarantined infected persons	$0.502(0.5 - 0.9)$	(Dénes et al., 2019.)
η_D Parameter for adjusting the transmissibility of people who died from Ebola	3.89	(Dénes et al., 2019.)
k Average per capita contact rate in the community	$9.15/week$	(Dénes et al., 2019.)
q Rate of quarantine of susceptible persons	$0.125(0.05 - 0.5)/\ week$	(Dénes et al., 2019.)
r_o Release rate from quarantine	$1.107(0.5 - 2)/\ week$	(Dénes et al., 2019.)

k_0^Q Average per capita contact rate during quarantine	$7.97/week$	(Dénes et al., 2019.)
$1/p$ Incubation period	$1.498\ week$	(Dénes et al., 2019.)
v Rate of recovery	$0.362/\ week$	(Dénes et al., 2019.)
m Rate of Ebola-induced death	$0.797/\ week$	(Dénes et al., 2019.)
w Rate of hospitalization	$1.58/week$	(Dénes et al., 2019.)
$1/f$ Average duration from death due to Ebola to burial	$0.762\ weeks$	(Dénes et al., 2019.)
ϕ_1 Vaccination rate of non-quarantined susceptible persons	$0.002(0-0.01)$	Assumed
ϕ_2 Vaccination rate of quarantined susceptible persons	$0.002(0-0.01)$	Assumed
ω Vaccine wear − off rate	$0.0191/$ week	(Brettin et al. 2018)
α_1 Inhibition rate by susceptible persons (quarantined)	$0.5/\ week$	Assumed
α_2 Inhibition rate due to quarantined symptomatic individuals	$0.2/\ week$	Assumed

The Model (3) is a modification of the Model for quarantine and isolation described by (Dénes et al., 2019.) among other things:

1. Individuals must be in the infectious compartment to infect others; this Model does not consider asymptomatic infections.
2. The infection is not vertically transmitted from the mother to the unborn baby.
3. Quarantine and vaccination were the intervention strategies used in the Model.
4. Quarantine implementation is assumed to be imperfect
5. Recovered individuals do not become infected again; there is no reinfection.
6. Treated (hospitalized) individuals can still transmit infection.

7. Infection-induced death occurs only in infectious compartments, and all compartments have the same natural death rate.
8. People need to be in the infectious compartment to infect others.

FINDINGS

Basic qualitative properties

Here, we present Model (3) 's fundamental qualitative properties, focusing on its solutions' non-negativity and boundedness.

Lemma 1: Assume that the initial values $S_U(0)$, $S_Q(0)$, $E_U(0)$,$E_Q(0)$,$V_U(0)$, $V_Q(0)$,$I_U(0)$, $I_T(0)$, $I_Q(0)$, $R(0)$, $D(0)$, and $B(0)$ are non-negative for model (3). Then, for all times $t > 0$, the solution to Equations (3) with these initial values will remain non-negative and bounded.

Proof: We will use a proof by contradiction to establish the non-negative nature of the solution. Suppose that, for the sake of contradiction, the claim is false. That is, assume there is a point $t = t^* \geq 0$ such that at $t = t^*$, at least one variable in Model (2) becomes negative, whereas all other variables in the Model are non-negative for $0 \leq t \leq t^*$. For instance, consider $S_U(t)$ as a state variable. If $S_U(t) = 0$, then $S_U'(t)$ is positive. Therefore, once $S_U(t)$ reaches 0, it cannot become negative. Similarly, the non-negativity of all other state variables can be proved using the same reasoning. It is helpful to define and demonstrate that the solutions of model (3) are bounded.

$$N(t) = S_U(t) + S_Q(t) + E_U(t) + E_Q(t) + V_U(t) + V_Q(t) + I_U(t) + I_T(t) + I_Q(t) + R(t) + D(t) \quad (5)$$

Let δ be defined as $\delta = \min\{f, d\}$. Therefore,

$$N'(t) = \Pi - d\big[S_U(t) + S_Q(t) + V_U(t) + V_Q(t) + E_U(t) + E_Q(t) + I_U(t) + I_T(t) + I_Q(t) + R(t)\big] - fD(t) \leq \Pi - \delta N(t) \quad (6)$$

Which implies $\limsup_{t\to\infty} N(t) \leq \frac{\Pi}{\delta}$. Since all solutions of the Model are non-negative, the second part of the lemma is proven. The feasible region for model (3) is defined as follows:

$$\Gamma = \{\big(S_U(t), S_Q(t), V_U(t), V_Q(t), E_U(t), E_Q(t), I_U(t), I_T(t), I_Q(t), R(t), D(t)\big) \in \mathbb{R}_+^{11}: N(t) \leq \frac{\Pi}{\delta}\} \quad (7)$$

From the preceding analysis, the following result can be inferred.

Lemma 2. For model (3), with any non-negative initial condition in $\mathbb{R}_+^{11}$, the region mentioned above Γ is positively invariant.

Disease-Free Equilibrium (DFE)

To determine the DFE of the Model (3), we consider the disease-free system corresponding to this Model, which is defined as:

$$S_U'(t) = \Pi - \phi_1 S_U(t) + \omega V_U(t) - dS_U(t)$$
$$V_U'(t) = \phi_1 S_U(t) - \omega V_U(t) - dV_U(t) \quad (8)$$

When all other state variables are zero, i.e.

$$S_Q(t) = E_U(t) = E_Q(t) =, V_Q(t) = I_U(t) = I_T(t) = I_Q(t) = R(t) = D(t) = 0 \quad (9)$$

Then, the fixed points of the disease-free system (3) can be determined as follows:

$$\Pi - \phi_1 S_U(t) + \omega V_U(t) - dS_U(t) = 0$$
$$\Phi_1 S_U(t) - \omega V_U(t) - dV_U(t) = 0 \quad (10)$$

Solving the system of equation (4) yields:

$$S_U(t) = \frac{(\omega + d)\Pi}{d(\phi_1 + \omega + d)}, \text{and } V_U(t) = \frac{\phi_1 \Pi}{d(\phi_1 + \omega + d)}$$

Hence, let $\varepsilon_0 = (S_U^*, 0,0,0, V_U^*, 0,0,0,0,0,0)$ denote the (DFE) of (3):

$$\varepsilon_0 = \left(\frac{(\omega + d)\Pi}{d(\phi_1 + \omega + d)}, 0,0,0, \frac{\phi_1 \Pi}{d(\phi_1 + \omega + d)}, 0,0,0,0,0,0\right) \quad (11)$$

Stability of DFE and $\mathcal{R}_0$

To calculate $\mathcal{R}_0$ and prove the local stability of the DFE for model (3), we utilize the Next-Generation Matrix (NGM) approach described by (Diekmann et al., 2010). The infection compartments in the Model (3) are E_U, E_Q, I_U, I_Q, and D. The disease-free compartments are S_U, S_Q, V_U, V_Q and R. The next-generation matrices, including V, for the Model are provided as follows:

$$NGM = \begin{pmatrix} 0 & 0 & \frac{bk(1-q)(d+\omega)}{d+\omega+\phi_1} & \frac{bk(1-q)(d+\omega)\eta_T}{d+\omega+\phi_1} & \frac{bkq(d+\omega)\eta_Q}{d+\omega+\phi_1} & \frac{bk(1-q)(d+\omega)\eta_D}{d+\omega+\phi_1} \\ 0 & 0 & \frac{bkq(d+\omega)}{d+\omega+\phi_1} & \frac{bkq(d+\omega)\eta_T}{d+\omega+\phi_1} & \frac{bkq(d+\omega)\eta_Q}{d+\omega+\phi_1} & \frac{bkq(d+\omega)\eta_D}{d+\omega+\phi_1} \\ 0 & 0 & 0 & 0 & 0 & 0 \\ 0 & 0 & 0 & 0 & 0 & 0 \\ 0 & 0 & 0 & 0 & 0 & 0 \\ 0 & 0 & 0 & 0 & 0 & 0 \end{pmatrix}, \text{and}$$

$$V = \begin{pmatrix} d+p & 0 & 0 & 0 & 0 & 0 \\ 0 & d+p & 0 & 0 & 0 & 0 \\ -p & 0 & d+m+v+w & 0 & 0 & 0 \\ 0 & 0 & -w & d+m+v & -w & 0 \\ 0 & -p & 0 & 0 & d+m+v+w & 0 \\ 0 & 0 & -m & -m & -m & f \end{pmatrix}$$

To estimate the basic reproductive value,R_0 defined as $R_0 = \rho(FV^{-1})$, we first need to calculate the matrix V^{-1}. Matrix $V^{-1} = (A_{6\times3} \quad B_{6\times3})$ is given by:

$$A = \begin{pmatrix} \frac{1}{d+p} & 0 & 0 \\ 0 & \frac{1}{d+p} & 0 \\ \frac{p}{(d+p)(d+m+v+w)} & 0 & \frac{1}{d+m+v+w} \\ \frac{p}{(d+p)(d+m+v)(d+m+v+w)} & \frac{pw}{(d+p)(d+m+v)(d+m+v+w)} & \frac{w}{(d+m+v)(d+m+v+w)} \\ 0 & \frac{mp}{(d+p)(d+m+v+w)} & 0 \\ \frac{mp}{f(d+p)(d+m+v)} & \frac{m}{f(d+p)(d+m+v)} & \frac{m}{f(d+m+v)} \end{pmatrix}, \text{ and}$$

$$B = \begin{pmatrix} 0 & 0 & 0 \\ 0 & 0 & 0 \\ 0 & 0 & 0 \\ \frac{1}{d+m+v} & \frac{w}{(d+m+v)(d+m+v+w)} & 0 \\ 0 & \frac{1}{d+m+v+w} & 0 \\ \frac{m}{f(d+m+v)} & \frac{m}{f(d+m+v)} & \frac{1}{f} \end{pmatrix}$$

Mathematica was used to perform the computations. Similarly, we can compute the matrix FV^{-1} and determine its spectral radius, which gives us the reproduction number. Therefore, $\mathcal{R}_0$ for Model (2) can be obtained as

$$\mathcal{R}_0 = \frac{bkp(d+\omega)\big(m(d+m+v+w)\eta_D + f(d+m+v)\big(1-q+q\eta_Q\big) + fw\eta_T\big)}{f(d+p)(d+m+v)(d+m+v+w)(d+\omega+\phi_1)}$$

Which can be written as,

$$\mathcal{R}_0 = \frac{bkp\left(m\eta_D(m+v+w+d) + qf\big(m\eta_Q + v\eta_Q + d\eta_Q + w\eta_T\big) + (1-q)f(m+v+w\eta_T+d)\right)(d+\omega)}{f(d+p)(d+m+v)(d+m+v+w)(d+\omega+\phi_1)}$$

Lemma 3: If $\mathcal{R}_0 < 1$, the DFE of the Model (3), as specified by (11), is LAS. Conversely, if $\mathcal{R}_0 > 1$, DFE becomes unstable.

According to this lemma, if the initial values of the state variables are within the region of attraction of the DFE (ε_0), the infection can be eliminated from the community when the fundamental reproductive value is less than one ($\mathcal{R}_0 < 1$).

Backward bifurcation analysis

In this part, we will establish the Endemic Steady State (EE) presence for model (3). We employ the center manifold theory to demonstrate that when $\mathcal{R}_0 = 1$, model (3) undergoes backward branching. We substituted the following variables:

$S_U(t) = y_1$, $S_Q(t) = y_2$, $E_U(t) = y_3$, $E_Q(t) = y_4$, $V_U(t) = y_5$, $V_Q(t) = y_6$, $I_U(t) = y_7$, $I_T(t) = y_8$, $I_Q(t) = y_9$, $R(t) = y_{10}$, and $D(t) = y_{11}$. Additionally, let

$$Y = (y_1, y_2, y_3, y_4, y_5, y_6, y_7, y_8, y_9, y_{10}, y_{11})^T$$

Therefore, model (3) can be represented as $\frac{dY}{dt} = G(Y)$, where

$$G = (g_1, g_2, g_3, g_4, g_5, g_6, g_7, g_8, g_9, g_{10}, g_{11})$$

Hence,

$$\frac{dy_1}{dt} = g_1 = \Pi - kby_1\lambda - qk(1-b)y_1\lambda + r_Q y_2 - \phi_1 y_1 + \omega y_5 - dy_1$$

$$\frac{dy_2}{dt} = g_2 = qk(1-b)y_1\lambda - \frac{bk_Q^Q y_2 y_9}{(1+\alpha_1 y_2)(1+\alpha_2 y_9)} - r_Q y_2 - \phi_2 y_2 + \omega y_6 - dy_2$$

$$\frac{dy_3}{dt} = g_3 = (1-q)kby_1\lambda - py_3 - dy_3$$

$$\frac{dy_4}{dt} = g_4 = qkby_1\lambda + \frac{bk_Q^Q y_2 y_9}{(1+\alpha_1 y_2)(1+\alpha_2 y_9)} - py_4 - dy_4$$

$$\frac{dy_5}{dt} = g_5 = \phi_1 y_1 - \omega y_5 - dy_5$$

$$\frac{dy_6}{dt} = g_6 = \phi_2 y_2 - \omega y_6 - dy_6 \qquad (12)$$

$$\frac{dy_7}{dt} = g_7 = py_3 - (v+m+w)y_7 - dy_7$$

$$\frac{dy_8}{dt} = g_8 = w(y_7 + y_9) - (v+m)y_8 - dy_8$$

$$\frac{dy_9}{dt} = g_9 = py_4 - (v+m+w)y_9 - dy_9$$

$$\frac{dy_{10}}{dt} = g_{10} = v(y_7 + y_8 + y_9) - dy_{10}$$

$$\frac{dy_{11}}{dt} = g_{11} = m(y_7 + y_8 + y_9) - fy_{11}$$

Where,

$$\lambda = \frac{y_7 + \eta_T y_8 + \eta_Q y_9 + \eta_D y_{11}}{y_1 + y_3 + y_5 + y_7 + y_8 + y_{10} + y_{11}}$$

The Jacobian matrix of system (12) at the corresponding disease-free equilibrium (ε_0) is expressed as:

$$J(\varepsilon_0) = [M_{11\times 6} \quad U_{11\times 6}]$$

Where,

$$M = \begin{pmatrix} -d-\phi_1 & r_Q & 0 & 0 & \omega & 0 \\ 0 & -d-r_Q-\phi_2 & 0 & 0 & 0 & \omega \\ 0 & 0 & -d-p & 0 & 0 & 0 \\ 0 & 0 & 0 & -d-p & 0 & 0 \\ \phi_1 & 0 & 0 & 0 & -d-\omega & 0 \\ 0 & \phi_2 & 0 & 0 & 0 & -d-\omega \\ 0 & 0 & p & 0 & 0 & 0 \\ 0 & 0 & 0 & 0 & 0 & 0 \\ 0 & 0 & 0 & p & 0 & 0 \\ 0 & 0 & 0 & 0 & 0 & 0 \\ 0 & 0 & 0 & 0 & 0 & 0 \end{pmatrix}$$, and

$$U = \begin{bmatrix} \frac{k(b(-1+q)-q)y_1^*}{y_1^*+y_5^*} & \frac{k(b(-1+q)-q)\eta_T y_1^*}{y_1^*+y_5^*} & \frac{k(b(-1+q)-q)\eta_Q y_1^*}{y_1^*+y_5^*} & 0 & \frac{k(b(-1+q)-q)\eta_D y_1^*}{y_1^*+y_5^*} \\ \frac{k(1-b)qy_1^*}{y_1^*+y_5^*} & \frac{k(1-b)q\eta_T y_1^*}{y_1^*+y_5^*} & \frac{k(1-b)q\eta_Q y_1^*}{y_1^*+y_5^*} & 0 & \frac{k(1-b)q\eta_D y_1^*}{y_1^*+y_5^*} \\ \frac{kb(1-q)y_1^*}{y_1^*+y_5^*} & \frac{kb(1-q)\eta_T y_1^*}{y_1^*+y_5^*} & \frac{bk(1-q)\eta_Q y_1^*}{y_1^*+y_5^*} & 0 & \frac{bk(1-q)\eta_D y_1^*}{y_1^*+y_5^*} \\ \frac{bkqy_1^*}{y_1^*+y_5^*} & \frac{bkq\eta_T y_1^*}{y_1^*+y_5^*} & \frac{bkq\eta_Q y_1^*}{y_1^*+y_5^*} & 0 & \frac{bkq\eta_D y_1^*}{y_1^*+y_5^*} \\ 0 & 0 & 0 & 0 & 0 \\ 0 & 0 & 0 & 0 & 0 \\ -d-m-v-w & 0 & 0 & 0 & 0 \\ w & -d-m-v & w & 0 & 0 \\ 0 & 0 & -d-m-v-w & -d & 0 \\ v & v & v & 0 & 0 \\ m & w & m & & -f \end{bmatrix}$$

Let's consider the case where $\mathcal{R}_0 = 1$. Let $(b \cdot k)$ be a bifurcation parameter. Solving for $\beta^* = b \cdot k$ gives:

$$\beta^* = \frac{f(d+p)(d+m+v)(d+m+v+w)(d+\omega+\phi_1)}{p\big(m\eta_D(m+v+w+d)+qf\big(m\eta_Q+v\eta_Q+d\eta_Q+w\eta_T\big)+(1-q)f(m+v+w\eta_T+d)(d+\omega)}$$

Near $b \cdot k = \beta^*$, system dynamics can be analyzed using center manifold theory. This is because at $b \cdot k = \beta^*$, all eigenvalues of the linearization matrix of the transformed system (6), except for one with a zero real part, have negative real parts. We obtain the right eigenvector $w = (w_1, w_2, \dots, w_{11})^T$ of $J(\varepsilon_0)|_{\beta^*}$ as follows:

$$w_1 = \frac{Q_1}{dmp(S^*+V^*)(d+\omega+\phi_1)(d+m+v+w)\big((d+\omega)\big(d+r_Q\big)+d\phi_2\big)}$$

With,

$$\begin{aligned} Q_1 = (d+\omega)(S^*(d(d+\omega+\phi_2)(f(q-1)(d+m+v)(d^2+d(m+p+v+w)+p(kq \\ +m+v+w))-kpq\big(m\eta_D(d+m+v+w)+fq\eta_Q(d+m+v)+fw\eta_T\big)\big)-f \\ (d+p)(d+\omega)r_Q(d+m+v)(d+m+v+w)\big)+fV^*(d+p)(d+m+v)(d+m \\ +v+w)\big(d(q-1)(d+\omega+\phi_2)+(-d-\omega)r_Q\big)\big) \end{aligned}$$

Similarly,

$$w_2 = -\frac{Q_2}{mp(S^* + V^*)(d+m+v+w)\big((d+\omega)\big(d+r_Q\big)+d\phi_2\big)}$$

With,

$$\begin{aligned}Q_2 =& q(d+\omega)(S^*(f(d+m+v)(d^2+d(m+p+v+w)+p(k(q-1)+m+v+w))-\\ & kp\big(m\eta_D(d+m+v+w)+fq\eta_Q(d+m+v)+fw\eta_T\big)\big)+fV^*(d+p)(d+m+v)\\ & (d+m+v+w)).\end{aligned}$$

$$w_3 = -\frac{f(q-1)(d+m+v)}{mp},\ w_4 = \frac{fq(d+m+v)}{mp}.$$

$$w_5 = \frac{Q_3}{(d+\omega+\phi_1)\big(m\eta_D(d+m+v+w)+f(d+m+v)\big(q\eta_Q-q+1\big)+fw\eta_T\big)}$$

With,

$$\begin{aligned}Q_3 = \phi_1\Bigg(& -\frac{kqS^*(d+\omega+\phi_2)\big(m\eta_D(d+m+v+w)+f(d+m+v)\big(q\eta_Q-q+1\big)+fw\eta_T\big)^2}{m(S^*+V^*)(d+m+v+w)\big((d+\omega)\big(d+r_Q\big)+d\phi_2\big)}\\ & -\frac{fq(d+p)(d+\omega)\eta_D r_Q(d+m+v)(d+m+v+w)}{dp\big((d+\omega)\big(d+r_Q\big)+d\phi_2\big)}\\ & +\frac{f(q-1)(d+p)\eta_D(d+m+v)(d+m+v+w)}{dp}\\ & -\frac{f^2q(d+p)(d+\omega)r_Q(d+m+v)\big((d+m+v)\big(q\eta_Q-q+1\big)+w\eta_T\big)}{dmp\big((d+\omega)\big(d+r_Q\big)+d\phi_2\big)}\\ & +\frac{f^2(q-1)(d+p)(d+m+v)\big((d+m+v)\big(q\eta_Q-q+1\big)+w\eta_T\big)}{dmp}\Bigg)\end{aligned}$$

$$w_6 = -\frac{Q_4}{mp(S^*+V^*)(d+m+v+w)\big((d+\omega)\big(d+r_Q\big)+d\phi_2\big)}$$

With,

$$\begin{aligned}Q_4 =& q\phi_2(S^*(f(d+m+v)(d^2+d(m+p+v+w)+p(k(q-1)+m+v+w))-kp(m\eta_D\\ & (d+m+v+w)+fq\eta_Q(d+m+v)+fw\eta_T\big)\big)+fV^*(d+p)(d+m+v)(d+m+v+w)\big).\end{aligned}$$

$$w_7 = -\frac{f(q-1)(d+m+v)}{m(d+m+v+w)},\qquad w_8 = \frac{fw}{m(d+m+v+w)}$$

$$w_9 = \frac{fq(d+m+v)}{m(d+m+v+w)},\qquad w_{10} = \frac{fv}{dm},\ w_{11} = 1$$

Similarly, $J(\varepsilon_{01})|_{\beta^*}$ has a left eigenvector, v expressed as $v = (v_1, v_2, \dots, v_{11})^T$, such that

$$v_1 = v_2 = v_5 = v_6 = v_{10} = 0$$

And,

$$v_3 = \frac{mp(d+m+v+w)\big(m\eta_D(d+m+v+w)+f(d+m+w\eta_T+v)\big)}{Q_6}$$

$$v_4 = \frac{mp(d+m+v+w)\big(m\eta_D(d+m+v+w)+f\eta_Q(d+m+v)+fw\eta_T\big)}{Q_6}$$

$$v_8 = \frac{m(d+p)(d+m+v+w)\big(m\eta_D(d+m+v+w)+f\eta_Q(d+m+v)+fw\eta_T\big)}{Q_6}$$

$$v_9 = \frac{m(d+p)(d+m+v+w)\big(m\eta_D(d+m+v+w)+f\eta_Q(d+m+v)+fw\eta_T\big)}{Q_6}$$

$$v_{11} = \frac{m(d+p)\eta_D(d+m+v)(d+m+v+w)^2}{Q_6}$$

Where,

$$\begin{aligned}Q_6 =& m\eta_D(d+m+v+w)^2(d^2+d(2f+m+p+v)+f(m+p+v)+p(m+v))+f^2(q\\ &\eta_Q(d+m+v)^2(2d+m+p+v+w)-(q-1)(d+m+v)^2(2d+m+p+v+w)\\ &+w\eta_T(w(2d+m+p+v)+(d+m+v)(3d+m+2p+v)))\end{aligned}$$

Thus, the related bifurcation coefficient $a = \sum_{k,i,j=1}^{11} v_k w_i w_j \frac{\partial^2 g_k}{\partial y_i \partial y_j}(0,0)$ is given by:

$$\begin{aligned}a =& \frac{1}{(S^*+V^*)^2}2\beta^*(q-1)v_3(S^*(w_3+w_5+w_7+w_8+w_{10}+w_{11})-V^*w_1)(w_{11}\eta_D\\ &+w_9\eta_Q+w_8\eta_T+w_7\big)-2v_4\big(-V^*\big(2bk_Q^Q S^* w_2 w_9+\beta^* q w_1\big(w_{11}\eta_D+w_9\eta_Q+w_8\\ &\eta_T+w_7\big)\big)-bk_Q^Q(S^*)^2 w_2 w_9-bk_Q^Q(V^*)^2 w_2 w_9+\beta^* qS^* w_3\big(w_{11}\eta_D+w_9\eta_Q+w_8\\ &\eta_T+w_7\big)+\beta^* qS^* w_5\big(w_{11}\eta_D+w_9\eta_Q+w_8\eta_T+w_7\big)+\beta^* qS^* w_{11}w_7\eta_D+\beta^* qS^*\\ &w_{11}^2\eta_D+\beta^* qS^* w_8 w_{11}\eta_D+\beta^* qS^* w_{10}w_{11}\eta_D+\beta^* qS^* w_9 w_7\eta_Q+\beta^* qS^* w_8 w_9\eta_Q\\ &+\beta^* qS^* w_9 w_{10}\eta_Q+\beta^* qS^* w_9 w_{11}\eta_Q+\beta^* qS^* w_8 w_7\eta_T+\beta^* qS^* w_8^2\eta_T+\beta^* qS^*\\ &w_8 w_{10}\eta_T+\beta^* qS^* w_8 w_{11}\eta_T+\beta^* qS^* w_7^2+\beta^* qS^* w_8 w_7+\beta^* qS^* w_{10}w_7+\beta^* qS^* w_{11}w_7\end{aligned} \quad (13)$$

Since the DFE (ε_0) of model (3) is LAS, the bifurcation coefficient (b) in Theorem 1 for this Model is always positive $(b > 0)$. Thus, the sign of (a) can determine the direction bifurcation in the Model as $\mathcal{R}_0 = 1$, and the system (12) will experience backward bifurcation at $\mathcal{R}_0 = 1$, if a is positive.

Theorem 1. A positive bifurcation coefficient a, defined by equation (13), indicates that Model (6), or equivalently Model (3), experiences backward bifurcation at $\mathcal{R}_0 = 1$.

Remark 1. The left and right eigenvectors associated with the zero eigenvalues of $J(\varepsilon_0)|_{\beta^*}$, which is the Jacobian of the system (12), along with the bifurcation coefficient a given in equation (13), are provided below; utilizing the parameter values specified in Table 1, we derive:

$$w = (-3215.53, 4.80, 2.50, 0.35, -327.44, 0.48, 0.60, 0.94, 0.08, 1103.55, 1)^T$$

$$v = (0,0,0.18,0.16,0,0,0.18,0.17,0.16,0,0.19)^T, \text{ and } a = 0.0611806$$

Hence, for $\mathcal{R}_0 = 1$, model (3) experiences backward bifurcation.

Non-existence of backward bifurcation

Here, we analyzed the scenario in which model (3) loses its backward bifurcation property. Consider a specific case of the Model for $q = 0$, which is the quarantine-free Model given below:

$$\begin{aligned}
S_U'(t) &= \Pi - kbS_U(t)\lambda(t) - \phi_1 S_U(t) + \omega V_U(t) - dS_U(t)\\
E_U'(t) &= kbS_U(t)\lambda(t) - pE_U(t) - dE_U(t)\\
V_U'(t) &= \phi_1 S_U(t) - \omega V_U(t) - dV_U(t)\\
V_U'(t) &= \phi_1 S_U(t) - \omega V_U(t) - dV_U(t)\\
I_U'(t) &= pE_U(t) - (v + m + w)I_U(t) - dI_U(t)\\
I_T'(t) &= wI_U(t) - (v + m)I_T(t) - dI_T(t)\\
R'(t) &= v\big(I_U(t) + I_T(t)\big) - dR(t)\\
D'(t) &= m(I_U(t) + I_T(t)) - fD(t)
\end{aligned} \tag{14}$$

Where,

$$\lambda(t) = \frac{I_U(t) + \eta_T I_T(t) + \eta_D D(t)}{N_U(t)}$$

We apply the center manifold method to demonstrate that the bifurcation direction for model (14) is forward when the reproduction number is one. When $q = 0$, Model (3) no longer exhibits the backward bifurcation property. For model (12), the primary reproductive value and the DFE are defined as follows:

$$\varepsilon_{01} = (S_U^*, 0, V_U^*, 0,0,0,0)$$

$$S_U^* = \frac{(\omega + d)\Pi}{d(\phi_1 + \omega + d)}$$

$$V_U^* = \frac{\phi_1 \Pi}{d(\phi_1 + \omega + d)}$$

And,

$$\mathcal{R}_{01} = \frac{bkp\big(m\eta_D(m + v + w + d) + f(m + v + w\eta_T + d)\big)(d + \omega)}{f(d + p)(d + m + v)(d + m + v + w)(d + \omega + \phi_1)}$$

Let $(b \cdot k)$ be a bifurcation parameter. $\beta^* = b \cdot k$, can be obtained by solving $\mathcal{R}_{01} = 1$.

$$\beta^* = \frac{f(d + p)(d + m + v)(d + m + v + w)(d + \omega + \phi_1)}{p\big(m\eta_D(m + v + w + d) + f(m + v + w\eta_T + d)\big)(d + \omega)}$$

We demonstrated that when $b \cdot k = \beta^*$, all eigenvalues of the Jacobian Model (8) at the corresponding DFE, $J(\varepsilon_{01})|_{\beta^*}$ have negative real parts, except for one eigenvalue with a zero

real part. The left and right eigenvectors associated with this zero eigenvalue are expressed as the right eigenvector is given by $w = (w_1, w_2, \dots, w_7)^T$, where

$$w_1 = -\frac{f(d+p)(d+m+v)(d+\omega)}{dmp(d+\omega+\phi_1)},\ w_2 = \frac{f(d+m+v)}{mp}$$

$$w_3 = -\frac{f(d+p)(d+m+v)\phi_1}{dmp(d+\omega+\phi_1)},\ w_4 = \frac{f(d+m+v)}{m(d+m+v+w)}$$

$$w_5 = \frac{fw}{m(d+m+v+w)},\ w_6 = \frac{fv}{dm},\ w_7 = 1$$

The left eigenvector is represented as $v = (v_1, v_2, \dots, v_7)^T$, where

$$v_1 = v_3 = v_6 = 0, \text{ and } v_2, v_4, v_5, v_7 > 0$$

Consequently, the bifurcation coefficient (a) associated with Theorem 1 is defined as follows:

$$a = -\frac{\begin{array}{r}2\beta^* v_2(d+\omega)(dm(df+mp+f(m+p+v))(d+m+v+w)\eta_D + f(d^2 f + \\ dmp + fpv + df(m+p+v)(d+m+v+w\eta_T)\big)\end{array}}{m^2 p(d+m+v+w)\pi(d+\omega+\phi_1)}$$

This implies that $a < 0$. According to Theorem 1, the disease-free equilibrium (ε_{01}) of Model (8) is locally asymptotically stable when $\mathcal{R}_{01} < 1$. Consequently, this indicates that the bifurcation coefficient b is more significant than zero. Therefore, in the quarantine-free Model, the bifurcation direction was forward. This implies that the backward bifurcation characteristic of Model (3) is lost when $q = 0$, allowing for the global stability of the DFE. Thus, imperfect (leaky) quarantine in Model (3) leads to backward bifurcation.

Remark 2. Using the center manifold approach, we have shown that Model (3) experiences backward bifurcation when $\mathcal{R}_0 = 1$. This phenomenon implies that even when the reproductive number $\mathcal{R}_0$ is less than one, an unstable (EE) and a stable (DFE) can coexist. This phenomenon arises from imperfect quarantine and indicates that while $\mathcal{R}_0 < 1$ is necessary for adequate infection; it is no longer sufficient. In other words, backward bifurcation caused by quarantine creates additional challenges for effectively controlling Ebola. The analysis demonstrated that backward bifurcation, absent in the quarantine-free Model (12), appears when imperfect quarantine is introduced.

Analyzing Uncertainty and sensitivity

The parameter values estimated in the model simulations are subject to uncertainties, considering that Model (3) includes several parameters. To address this uncertainty, we conducted an analysis using LHS (Latin Hypercube Sampling) with $\mathrm{N} = 10000$ runs. In this analysis, we assumed each parameter followed a uniform distribution, utilizing the parameter ranges provided in Table 1.

The results of the uncertainty analysis, with $\mathcal{R}_0$ as the response function with $q = 0$, and $\phi_1 = 0$ (i.e., without considering quarantine and vaccination) shows that the 95% Confidence interval for $\mathcal{R}_0$ is $[0.2,3.62]$, with a mean value of 1.17. When only quarantine was

used as an intervention strategy (i.e.,$\phi_1 = 0$), the 95% confidence interval for $\mathcal{R}_0$ was $[0.2,3.41]$, with a mean value of 1.12. This indicates a slight reduction in the reproduction number; however, it remains above unity.

When vaccination is considered an intervention strategy (with $q = 0$, meaning no quarantine), the uncertainty analysis results in a 95% confidence interval for the reproduction number of $[0.0001,0.0014]$, with a mean value of 0.00044. This indicates that vaccinating non-quarantined susceptible individuals significantly impacts the infection burden and can lower the reproductive value to less than one.

To identify the parameters that most affect the dynamics of the infection, a sensitivity analysis was conducted using the PRCC (Partial Rank Correlation Coefficients) method. This analysis ranks the influence of parameters based on how they vary within their associated ranges, using the commutative number of new Ebola cases as the outcome (response function).

The analysis revealed that the quarantine effectiveness parameter (η_Q), and the parameter about the isolation of those who are vulnerable persons (q) had less influence on the incidence of new Ebola cases. Furthermore, the simulation indicated that the hospitalization rate of individuals had the highest negative partial rank correlation coefficient, suggesting that it had the greatest negative effect on the outcome.

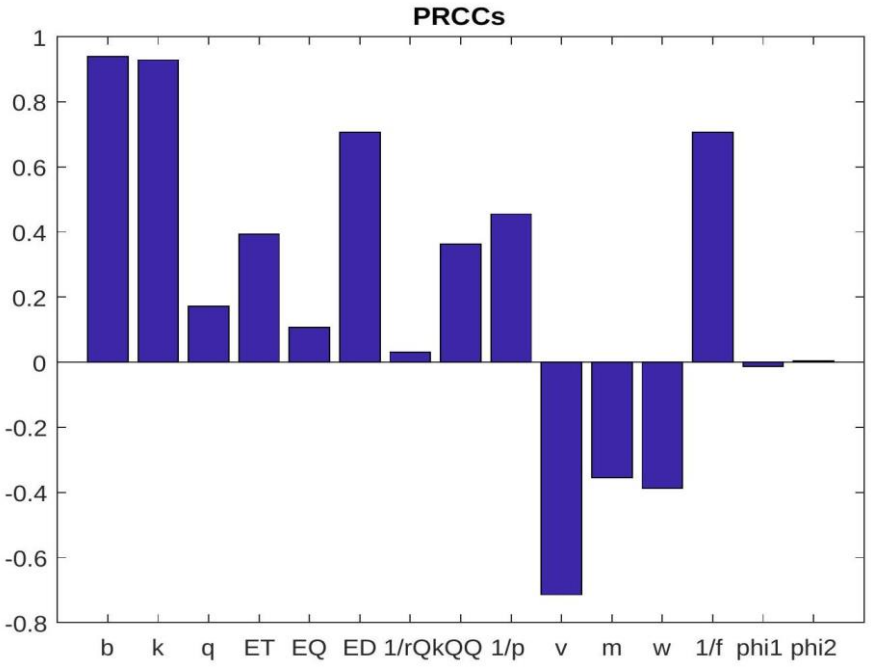

Figure 2. Plot of sensitivity analysis for the basic reproduction value $\mathcal{R}_0$.

The PRCCs bar chart is used for sensitivity analysis of the model parameters to understand their influence on the model output. The height of each bar indicates the strength of the correlation between the parameter and the model output. Parameters with taller bars have a stronger influence on the model outcomes.

Numerical Simulations

To further examine the transfer dynamics of the Ebola virus and determine the influence of vaccination and isolation measures on the community, we performed numerical simulations of the Model. These simulations were conducted using the Mathematica software, with the parameter values listed in Table 1. These simulations revealed that vaccinating susceptible individuals, particularly non-quarantined susceptible individuals (ϕ_1), had the most significant influence on the burden of infection (Figures 4 and 5), the quarantine rate of vulnerable people (q), and the average quarantine duration $(1/r_Q)$ significantly affected the number of Ebola cases (Figures 3 and 6). Conversely, Figures 7 and 8 demonstrate that the contact rate during quarantine (η_Q) has a marginal influence on infection obligation.

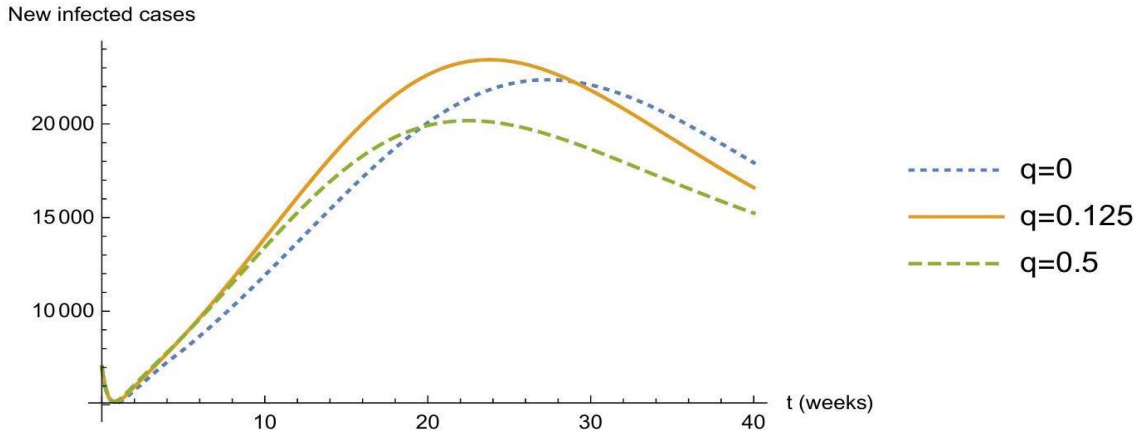

Figure 3. Illustrates how various quarantine rates q for vulnerable individuals influence the incidence of new Ebola cases.

The figure demonstrates that higher quarantine rates for vulnerable individuals lead to decreased peak and overall incidence of new Ebola cases. Increased quarantine rates effectively lower disease spread among vulnerable populations.

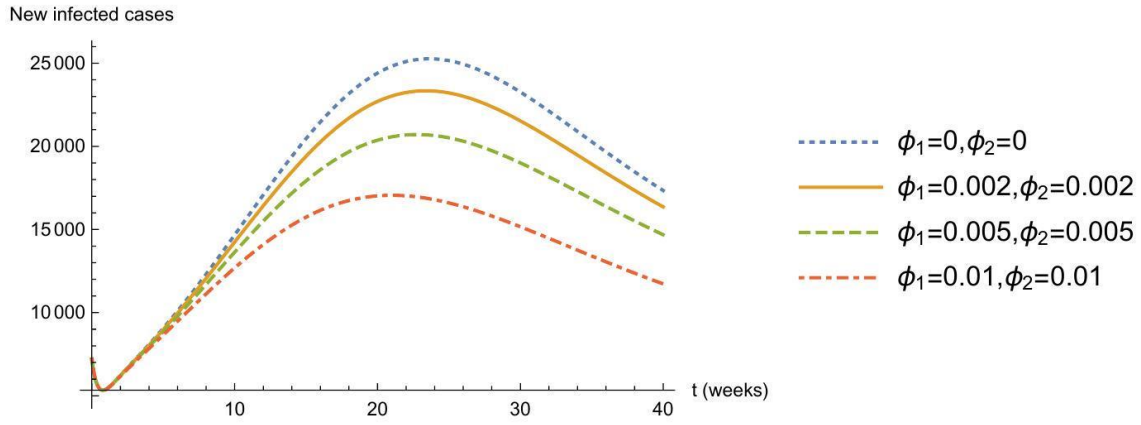

Figure 4. Illustrates the effect of varying vaccination rates $(\phi_1, and\ \phi_2)$ for non-quarantined and quarantined vulnerable individuals, respectively, on the incidence of new Ebola cases.

The figure shows how vaccination rates for non-quarantined and quarantined individuals affect new case incidence. Higher vaccination rates, especially among non-quarantined individuals, are more effective in decreasing new cases.

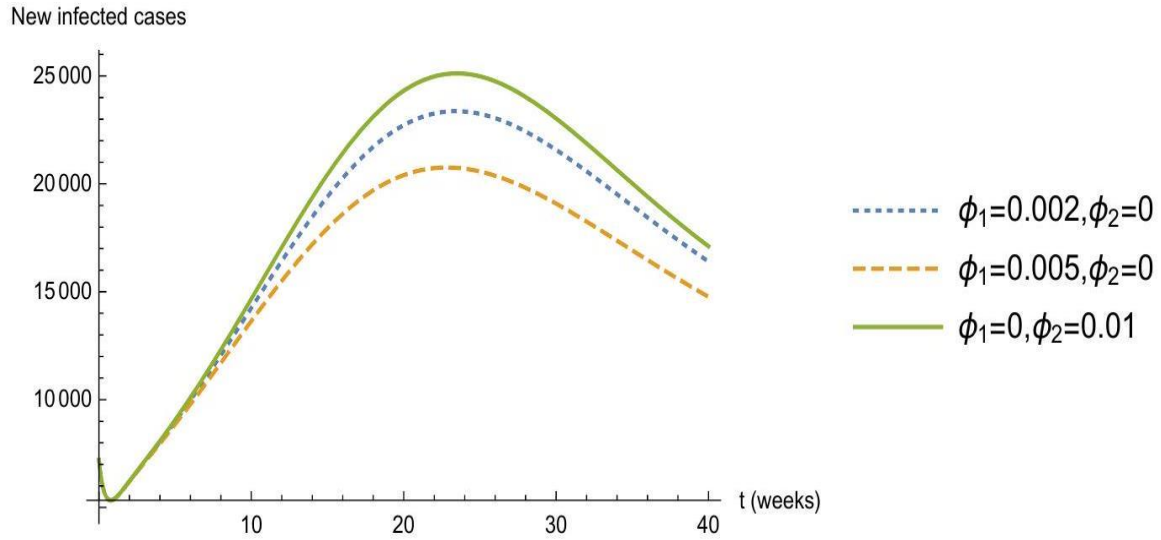

Figure 5. Demonstrates the comparative effect of different vaccination rates (ϕ_1, ϕ_2)—for non-quarantined and quarantined vulnerable people, respectively, on the incidence of new Ebola cases.

The figure illustrates that vaccinating non-quarantined individuals (blue and yellow lines) lowers peak Ebola cases more than vaccinating quarantined individuals (green line). The lowest peak is when non-quarantined individuals have the highest vaccination rate.

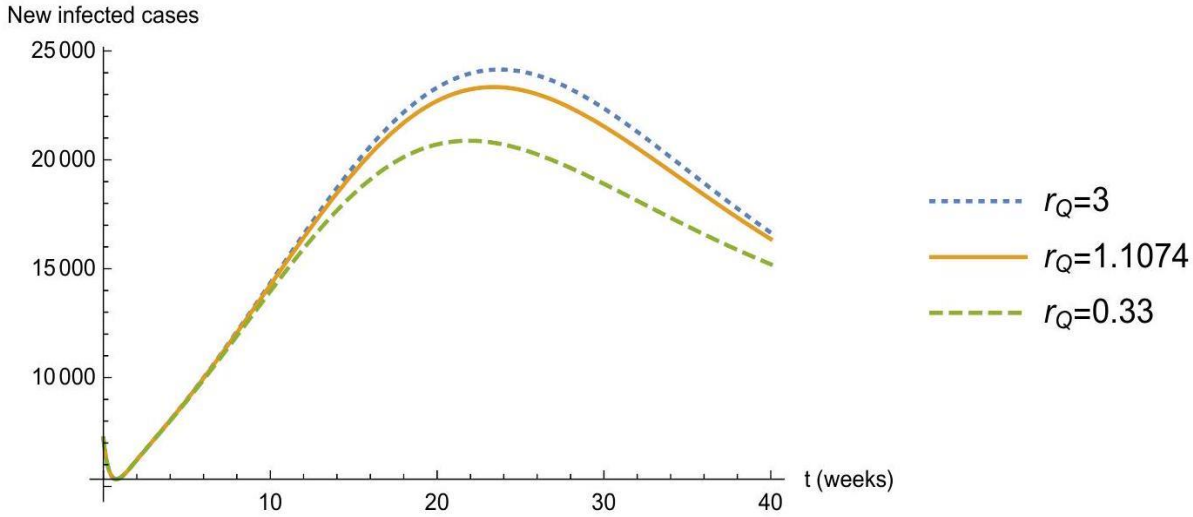

Figure 6. Demonstrates the influence of the quarantine duration $(1/r_Q)$ and varying release rates from quarantine (r_Q) on the incidence of new Ebola cases

This figure shows that shorter quarantine durations (higher. r_Q) lead to higher peaks of new cases, while longer durations (lower r_Q) result in a lower peak and quicker decline. This highlights the importance of appropriate quarantine duration to control the spread of Ebola.

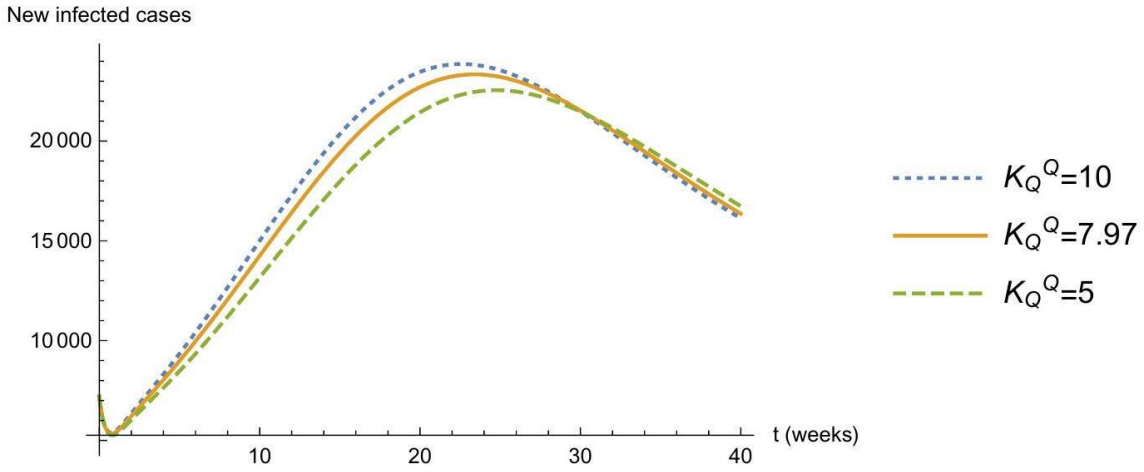

Figure 7. Illustrates the influence of varying per capita contact rates in quarantine (k_Q^Q) on the incidence of new Ebola cases.

The figure indicates that higher per capita contact rates within quarantine settings lead to higher peaks and a more prolonged incidence of new cases. Reducing contact rates in quarantine can significantly decrease the spread of the disease.

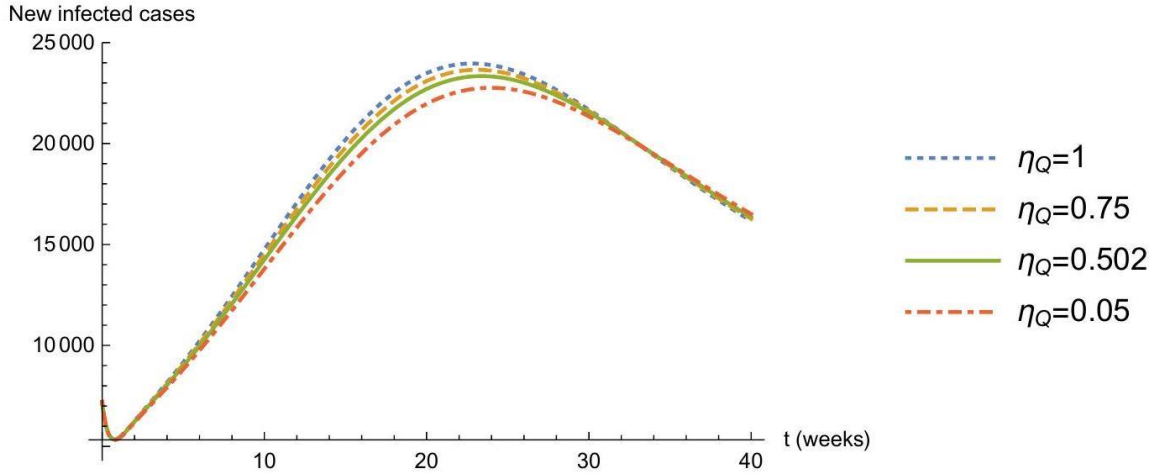

Figure 8. Illustrates the influence of varying rates of (η_Q), the parameter modifies infectiousness during quarantine on the incidence of new Ebola cases

This figure demonstrates that decreasing the parameter η_Q, which modifies infectiousness during quarantine and reduces the peak and total number of new cases. Lower η_Q values make quarantine more effective in controlling the disease spread.

DISCUSSION

The quarantine and vaccination of people suspected of exposure to infectious diseases have historically been key public health measures to combat the spread of these diseases. In this study, we developed the SEIQRD deterministic model established by Dénes et al. (2019) to evaluate the population-level effects of quarantine and vaccination on individuals potentially exposed to the Ebola virus. Some of the Key features of the Model include the explicit representation of quarantine for both susceptible and infected individuals (following the approach of Dénes et al., (2019)), the assumption that quarantine is not perfectly

effective (allowing for disease transmission during quarantine), and introducing two new compartments for vaccinated individuals: one for those who are quarantined and the other for those who are not quarantined. Unlike the Model demonstrated by Dénes et al. (2019), which uses a standard incidence rate of infection (for quarantined individuals), we employed a monotone nonlinear incidence rate (Crowley-Martin type). This approach models the rate at which new cases occur over time rather than the cumulative number of cases, thereby accounting for the inhibitory effects of behavioral changes among susceptible and infected individuals as their numbers increase.

A detailed theoretical analysis of the stability of the disease-free equilibrium was performed. The analysis revealed that the disease-free equilibrium of the Model is locally asymptotically stable when the basic reproductive value of the Model ($\mathcal{R}_0$) is smaller than one. The epidemiological implication of this result is that if the initial values of the state variables are within the region of attraction of disease-free equilibrium, the infection can be eliminated from the community when the basic reproductive value is less than one. However, if $\mathcal{R}_0$ is greater than one, the DFE becomes unstable, indicating that the infection will persist in the population.

Our analysis indicates that the bifurcation direction is forward without quarantine measures, demonstrating the absence of backward bifurcation. This finding suggests that the disease-free equilibrium (DFE) remains globally stable, allowing for effective disease eradication. However, introducing imperfect or leaky quarantine in Model (3) results in backward bifurcation, leading to potential disease persistence despite the basic reproductive number being below one. This scenario indicates that while $\mathcal{R}_0 < 1$ is critical for adequate infection; it is insufficient for disease control. Consequently, the backward bifurcation stemming from quarantine complicates the effective management of Ebola.

A detailed uncertainty analysis conducted using Latin Hypercube Sampling (LHS) with 10,000 simulations elucidated the impact of parameter variability on the primary reproduction number and the effectiveness of different intervention strategies. In the absence of interventions, the 95% confidence interval for $\mathcal{R}_0$ spans from 0.2 to 3.62, with a mean of 1.17, indicating substantial uncertainty in the potential for disease spread. Introducing quarantine as the sole intervention reduces the confidence interval to $[0.2,3.41]$ and lowers the mean $\mathcal{R}_0$ to1.12, reflecting a modest decrease but still leaving $\mathcal{R}_0$ above one. This finding suggests that quarantine alone is insufficient for disease elimination. However, incorporating vaccination significantly lowers $\mathcal{R}_0$, with the 95% confidence interval narrowing to$[0.0001, 0.0014]$ and a mean of 0.00044, demonstrating its high effectiveness in reducing $\mathcal{R}_0$ below one and potentially ending the epidemic.

Sensitivity analysis using Partial Rank Correlation Coefficients (PRCC) identified critical parameters that significantly affect the incidence of new Ebola cases. Specifically, the analysis highlighted that the community contact rate (k), the transmission probability per contact (β), and the mean duration before the burial of Ebola-deceased individuals ($1/f$) were the most influential factors contributing to the disease burden. This finding

emphasizes the necessity of implementing targeted interventions aimed at reducing contact with suspected cases and minimizing burial delays to mitigate the spread of Ebola effectively. However, the analysis indicated that the effectiveness of quarantine (η_Q) and the duration of quarantine had a smaller impact on the number of infections compared to the modified transmission rate during quarantine and the contact rates among quarantined individuals. However, the results suggest that quarantine remains a valuable tool for disease control if applied with sufficiently high coverage and effectiveness. However, quarantine measures may need to be supplemented with other strategies like vaccination to achieve adequate disease elimination.

CONCLUSION

In conclusion, the Model emphasizes the importance of vaccination in reducing Ebola virus transmission. The analysis demonstrated that quarantine measures alone may not be sufficient; however, combined with vaccination, they can significantly reduce infection rates. This highlights the enhanced efficacy of integrated strategies compared to isolated methods.

Consequently, control strategies must prioritize the enhancement of vaccination coverage. Additionally, reinforcing quarantine measures and limiting interactions during quarantine are crucial for decreasing viral transmission. These findings offer significant insights for policymakers, aiding in formulating effective intervention plans to manage and eradicate viral diseases.

REFERENCES

Alimi, A. A., & Ayoade, A. A. (2023). Mathematical modeling of the effect of vaccination on the dynamics of infectious diseases. *Nepal Journal of Mathematical Sciences*, *4*(1), 1–10. https://doi.org/10.3126/njmathsci.v4i1.53151

Bisimwa, P., Biamba, C., Aborode, A. T., Cakwira, H., & Akilimali, A. (2022). Ebola virus disease outbreak in the Democratic Republic of the Congo: A mini-review. *Annals of Medicine and Surgery*, *80*. https://doi.org/10.1016/j.amsu.2022.104213

Brabers, J. H. V. J. (2023). The spread of infectious diseases from a physics perspective. *Biology Methods and Protocols*, *8*(1). https://doi.org/10.1093/biomethods/bpad010

Brettin, A., Rossi–Goldthorpe, R., Weishaar, K., & Erovenko, I. V. (2018). Ebola could be eradicated through voluntary vaccination. *Royal Society Open Science*, *5*(1), 171591. https://doi.org/10.1098/rsos.171591

Castillo-Chavez, C., & Song, B. (2004). Dynamical models of tuberculosis and their applications. *Mathematical Biosciences & Engineering*, *1*(2), 361–404. https://doi.org/10.3934/mbe.2004.1.361

Dénes, A., & Gumel, A. B. (2019). Modeling the impact of quarantine during an outbreak of Ebola virus disease. *Infectious Disease Modelling*, *4*, 12–27. https://doi.org/10.1016/j.idm.2019.01.003

Desai, K., & Arora, P. (2023). Burden of infectious diseases and strategies of prevention. In *Elsevier eBooks* (pp. 49–61). https://doi.org/10.1016/b978-0-323-85730-7.00052-7

Diekmann, O., Heesterbeek, J. a. P., & Roberts, M. G. (2009). The construction of next-generation matrices for compartmental epidemic models. *Journal of the Royal Society Interface*, *7*(47), 873–885. https://doi.org/10.1098/rsif.2009.0386

Dubey, P., Dubey, B., & Dubey, U. S. (2016). An SIR Model with Nonlinear Incidence Rate and Holling Type III Treatment Rate. In *Springer proceedings in mathematics & statistics* (pp. 63–81). https://doi.org/10.1007/978-81-322-3640-5_4

Harris, P. J., & Bodmann, B. E. J. (2022). A mathematical model for simulating the spread of a disease through a country divided into geographical regions with different population densities. *Journal of Mathematical Biology*, *85*(4). https://doi.org/10.1007/s00285-022-01803-6

Isiaka, N. a. B., Anakwenze, N. V. N., Ilodinso, N. C. R., Anaukwu, N. C. G., Ezeokoli, N. C. M., Noi, N. S. M., Agboola, N. G. O., & Adonu, N. R. M. (2024). Harnessing artificial intelligence for early detection and management of infectious disease outbreaks. *International Journal of Innovative Research and Development*. https://doi.org/10.24940/ijird/2024/v13/i2/feb24016

Jain, S., Khaiboullina, S., Martynova, E., Morzunov, S., & Baranwal, M. (2023). Epidemiology of Ebolaviruses from an Etiological Perspective. *Pathogens*, *12*(2), 248. https://doi.org/10.3390/pathogens12020248

Liu, S. (2023). Disease mechanism and treatment method of Ebola virus. *Highlights in Science Engineering and Technology*, *45*, 116–121. https://doi.org/10.54097/hset.v45i.7331

Maldonado, Y. A. (2023). Lessons from a House on Fire—from smallpox to polio. *The Journal of Infectious Diseases*, *227*(9), 1025–1027. https://doi.org/10.1093/infdis/jiad017

Marino, S., Hogue, I. B., Ray, C. J., & Kirschner, D. E. (2008). A methodology for performing global uncertainty and sensitivity analysis in systems biology. *Journal of Theoretical Biology*, *254*(1), 178–196. https://doi.org/10.1016/j.jtbi.2008.04.011

Niyukuri, D., Sinigirira, K. J. G., De Dieu Kwizera, J., & Adam, S. O. A. (2023, June 3). *Ebola transmission dynamics: will future Ebola outbreaks become cyclic?* arXiv.org. http://arxiv.org/abs/2306.02075

Nurwijaya, S., Kurniati, R., MA, & Sugiarto, S. (2023). DYNAMICAL SYSTEM FOR EBOLA OUTBREAK WITHIN QUARANTINE AND VACCINATION TREATMENTS. *BAREKENG JURNAL ILMU MATEMATIKA DAN TERAPAN*, *17*(2), 0615–0624. https://doi.org/10.30598/barekengvol17iss2pp0615-0624

Pecoraro, F., Luzi, D., & Clemente, F. (2021). The efficiency in the ordinary hospital bed management: A comparative analysis in four European countries before the COVID-19 outbreak. *PLoS ONE*, *16*(3), e0248867. https://doi.org/10.1371/journal.pone.0248867

Rai, N. R., Sharma, N. A., & Negi, N. S. (2024). Emerging infectious diseases: a persistent threat to the community. *International Healthcare Research Journal*, *7*(12), RV17–RV20. https://doi.org/10.26440/ihrj/0712.03626

Sabaté, M. C. (2023). *Mathematical modelling to study infectious diseases: from understanding to prediction*. https://doi.org/10.5821/dissertation-2117-358138

Siddique, M. P. (2022). Coping with Contagious Diseases: A Global Perspective. *Journal of* Islamic International Medical College, 17(3), 148–151. https://doi.org/10.57234/1543

Samadi, A. (2024). Impacts of Climate Change on Vector-Borne Diseases of Animals and Humans with Special Emphasis on Afghanistan. Journal of Natural Science Review, 2(1), 1–20. https://doi.org/10.62810/jnsr.v2i1.35

Umutesi, G., Moon, T. D., Makam, J. K., Diomande, F., Cherry, C. B., Tuopileyi, R. N., II, Zakari, W., & Craig, A. S. (2023). Evaluation of acute flaccid paralysis surveillance performance before and during the 2014-2015 Ebola virus disease outbreak in Guinea and Liberia. *Pan African Medical Journal*, *45*. https://doi.org/10.11604/pamj.2023.45.190.21480